20/05/2013

Contrasting H-mode behaviour with fuelling and nitrogen seeding in the all-carbon and metallic versions of JET

G. Maddison [1], C. Giroud [1], M. Beurskens [1], S. Brezinsek [2], P. Devynck [3], T. Eich [4], S. Jachmich [5], A. Järvinen [6], C. Lowry [7], S. Marsen [4], K. McCormick [4], A. Meigs [1], F. Rimini [1], M. Stamp [1] and JET EFDA contributors [†]

JET-EFDA, Culham Science Centre, Abingdon, OX14 3DB, UK.

[1] *EURATOM/CCFE Fusion Association, Culham Science Centre, Oxon. OX14 3DB, UK.*
[2] *IEK-Plasmaphysik, FZ Jülich, Association EURATOM-FZJ, Jülich, Germany.*
[3] *CEA-Cadarache, Association Euratom-CEA, 13108 St Paul-lez-Durance, France.*
[4] *Max-Planck-Institut für Plasmaphysik, EURATOM-Association, 85748 Garching, Germany.*
[5] *Association Euratom-Etat Belge, ERM-KMS, Brussels, Belgium.*
[6] *Aalto University, Association EURATOM-Tekes, Otakaari 4, 02150 Espoo, Finland.*
[7] *JET-EFDA/CSU, Culham Science Centre, Abingdon, Oxon. OX14 3DB, UK.*

1. Introduction

An all-metal ITER-like wall (ILW) [1], consisting of beryllium in the main chamber and tungsten surfaces in the divertor, has now been installed in JET to pursue low retention of fuel species and to explore the impact on next-step-relevant plasmas. Its implementation has offered a unique opportunity to compare behaviour with that in the previous all-carbon lining, notably for high-triangularity Type I H-modes with impurity seeding, a technique recognised to be necessary for power handling both in ITER and in JET at full performance. Contrasting results are reported for closely-matched deuterium-fuelling plus nitrogen-seeding scans in each JET environment. Attention is focused upon neutral-beam-heated plasmas with total input power 15 - 17 MW at 2.65 T, 2.5 MA, $q_{95} \approx 3.5$, average triangularity $\delta \approx 0.4$, elongation $\kappa \approx 1.7$ and gas inputs spanning ranges $0.75 \leq \Phi_D \leq 3.3$, $0 \leq \Phi_N \leq 4.7$ (10^{22} electrons / s assuming full ionisation).

2. Density, purity and inter-ELM radiation fraction

At high triangularity in the all-C machine, H-mode density could be raised even slightly above Greenwald level by gas puffing without significantly degrading normalised energy confinement [2]. Injecting N into the divertor of such plasmas, however, led to a fall in density again, as shown by the open points in Fig. 1(a). On the other hand, unseeded pulses in the ILW began at ≈ 10% lower density for similar fuelling, but then conversely this increased as N was added (filled symbols). These exactly opposite responses of combined fuelling efficiency and particle confinement had important consequences e.g. for accompanying inter-ELM radiated power fraction, as seen in Fig. 1(b). In the all-C cases, $f_{\mathrm{rad}}^{\mathrm{i-E}}$ did not change monotonically, instead actually tending to drop at low N input owing to the loss of density, before rising again for stronger seeding, a variation best seen for higher fuelling. Against this, unseeded plasmas in the ILW achieved significantly lower intrinsic impurity content and so higher purity, as anticipated for an all-metal wall, with correspondingly lower inter-ELM radiation. Mounting N seeding then produced a steady increase in $f_{\mathrm{rad}}^{\mathrm{i-E}}$ until a level similar to that in the all-C scans was recovered, though still at Z_{eff} better than or equal to the best all-C instances. The apparent ceiling of $f_{\mathrm{rad}}^{\mathrm{i-E}} \approx 0.6$ in both environments remains below the

[†] *see appendix of F. Romanelli et al, Proceedings of the 24th IAEA Fusion Energy Conference, October 2012, San Diego, USA.*

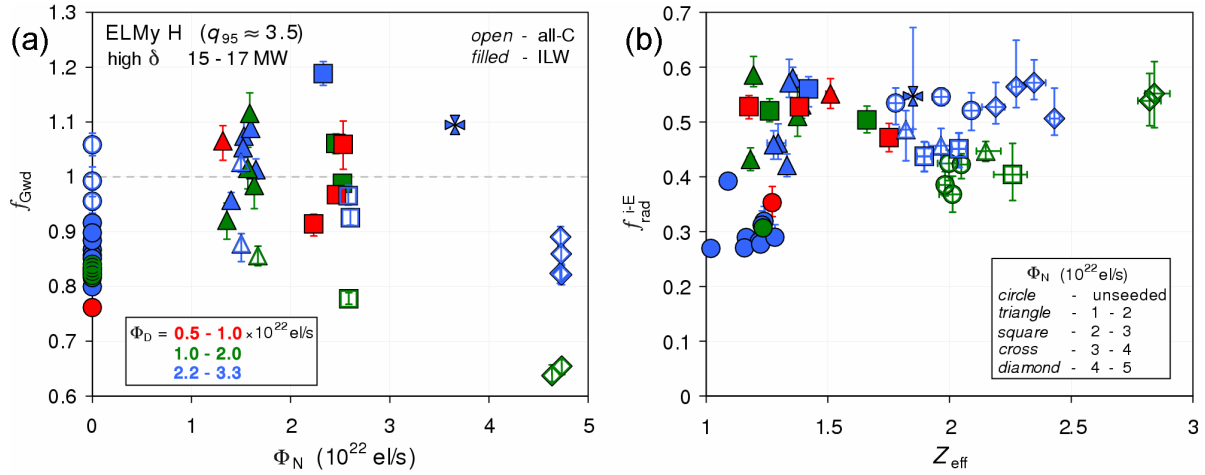

Fig. 1 (a) Normalised density versus N seeding rate. (b) Inter-ELM radiated power fraction versus line-average effective ionic charge (from visible bremsstrahlung). Points colour and symbol coded for D-fuelling and N-seeding rates respectively. Open symbols: all-C; filled symbols: ILW.

classically expected limit [3] for N edge emission, even allowing for departure from coronal equilibrium [4], and may pertain to a regime boundary rather than strict saturation.

3. Pedestal and confinement

Largely owing to the drop in density, N seeding in the all-C wall resulted in a reduced pedestal and consequent loss of normalised confinement, as disclosed in Fig. 2. Here electron edge profiles have been interpolated with a modified tanh function [5] fitted to high-resolution Thomson scattering data selected during the final third of inter-ELM periods within a 1 - 2 s flat-top window. In contrast, unseeded ILW counterparts had significantly lower (electron) pedestal pressure and ≈ 30% lower confinement, actually due to a commensurately cooler $T_e^{\text{ped i-E}}$. Progressively higher N input then induced a recovery in pedestal height and confinement, firstly due to the rise in density, but eventually involving an increase [6] even in $T_e^{\text{ped i-E}}$ for almost constant pressure. Both ILW and all-C environments finally realised approximately the same performance for similar fuelling and seeding levels. Best direct proportionality lines separately through each respective dataset reveal the same relationship between pedestal height and confinement was also preserved. Simultaneously, peaking of core (electron) pressure was almost invariant or even decreasing slightly towards higher confinement, affirming quality of the latter was unequivocally determined by the pedestal.

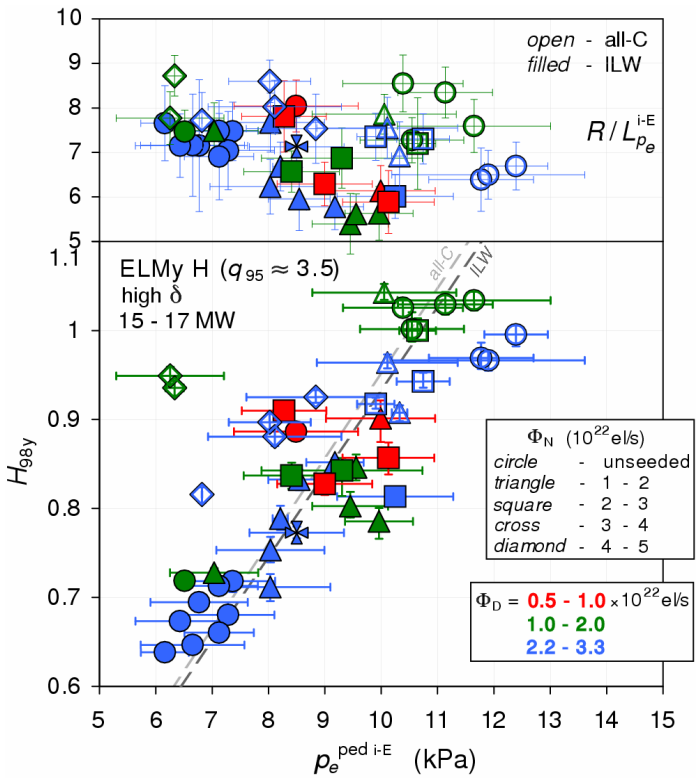

Fig. 2 Normalised energy confinement (bottom) and normalised core electron pressure gradient scale-length (top) versus inter-ELM electron pressure pedestal height. Key as in Fig. 1.

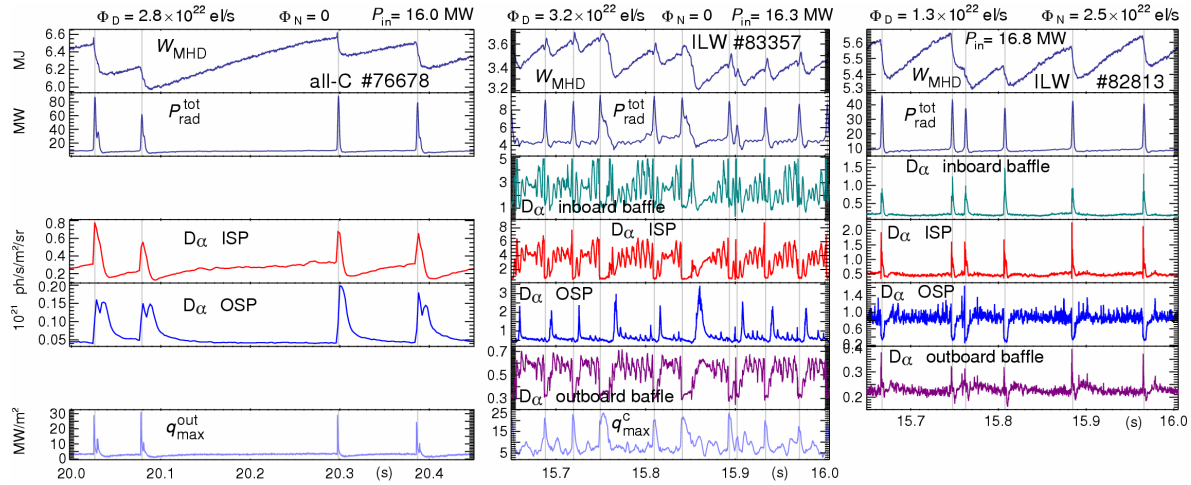

Fig. 3 (From top): stored energy, total radiated power, Dα emission from the inboard baffle, inboard strike-point, outboard strike-point and outboard baffle of the divertor, and power density on the outboard target from fast IR thermography. Examples of (left): unseeded all-C; (centre): unseeded ILW; (right): N-seeded ILW.

4. Divertor recycling

Recycling imposes a fundamental boundary condition on tokamak plasmas and would be expected to be particularly affected by the change from all-C to all-metal walls. Responses during Type I ELMing in the all-C machine are typified in Fig. 3 (left). Within measurement uncertainties, each ELM crash induced a rapid loss of stored energy with near coincident spikes in total radiation, recycling at the divertor inboard and outboard strike-points and heat load density at the latter detected by fast infra-red thermography. This pattern persisted either without or with N seeding. Radically different dynamics emerged in the ILW, however, where unseeded pulses (centre) now exhibited much slower ELM collapses [7], coupled with a drop in recycling at the ISP and both sides of the divertor entrance. Only at the OSP did a rise in recycling persist and then after a delay of several milliseconds, depending upon the ELM size. At both strike-points, average Dα emission was roughly 10× brighter than in the all-C situation for similar fuelling. In between ELMs, spontaneous oscillations [8] in ILW divertor recycling appeared (here at ~ 200 Hz), which also acted in in-out anti-phase. Adding N tended to recover the faster time-scale of ELM unload, suppress divertor oscillations and at higher levels to reverse the asymmetry of recycling, i.e. a prompt rise at the ISP and divertor entrance accompanied ELMs, while a fall occurred at the OSP. Symmetric behaviour as in the all-C divertor was thus not recovered. The extent to which altered recycling might contribute to changed ELM and confinement properties in the ILW remains under study.

5. Power balance

Impurity seeding is intended primarily to reduce heat loads on target surfaces by dispersing power as radiation. The balance firstly between ELMs has been estimated by averaging quantities over intervals 50 - 90% of the way between neighbouring peaks during 1 - 2 s flat-top windows. Fractional power load on the whole toroidal outboard target has been derived from fast IR thermography for all-C cases and, lacking this generally, from embedded Langmuir probes with a sheath transmission factor $\gamma = 8$ in the ILW. The latter data are divided into two sets with either good probe profiles (plain symbols), or some points missing (feint symbols) so that associated values can properly be regarded only as lower bounds. Results are plotted against inter-ELM exhaust fraction in Fig. 4, where it becomes clear that in the ILW, target load declined in proportion to the radiative cooling plus ELM recurrence ($\partial W^{\mathrm{i-E}}/\partial t$) effects of N injection. Discounting two outlying pulses which reverted to

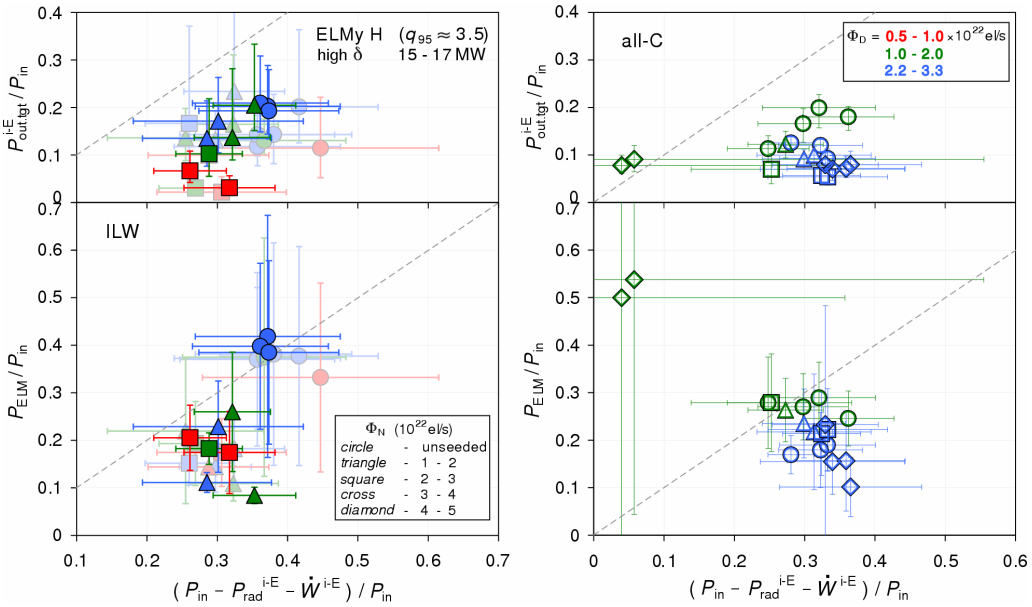

Fig. 4 Power fractions (top) landing on the outboard target between ELMs and (bottom) ejected in ELMs versus inter-ELM exhaust fraction. (Left): ILW (plain symbols: target probes best defining heat load; feint symbols: some probes missing); (right): all-C. Key as in Fig. 1.

Type III regime, a similar outcome prevailed in the all-C scans. By averaging ELM energy amplitude divided by the preceding inter-ELM period ($\Delta W^{ELM} / \Delta t^{i-E}$) over the same flat-top windows, an approximation of power efflux in these fluctuations can also be extracted. A priori a simple relation to inter-ELM exhaust would not necessarily be expected and this seems to have been borne out for the all-C plasmas. Surprisingly, though, ELM power fraction in the ILW again decreased roughly in proportion with the impact of N, adding a significant bonus to its use.

6. Summary

Replacing the former all-C wall in JET with all-metal surfaces has markedly changed the plasma boundary conditions and intrinsic impurity characteristics. Pedestal, confinement and ELM behaviour have all been found to be strongly affected. However, seeding with N has not only succeeded in reducing divertor heat loads, between and even at ELMs, but also beneficially recovered much of the all-C performance by helping to raise plasma density and, for the first time in JET, electron pedestal temperature. Attention in next experiments is on controlling W contamination, improving stationarity and testing noble gases further to extend development of a full-power, long-pulse H-mode scenario.

This work, part-funded by the European Communities under the contract of Association between EURATOM/CCFE and by the RCUK Energy Programme [grant number EP/I501045], was supported by EURATOM and carried out within the framework of the European Fusion Development Agreement. The views and opinions expressed herein do not necessarily reflect those of the European Commission.

References

[1] G. F. Matthews *et al* Physica Scripta **T128** (2007) 137
[2] A. Loarte *et al* Plasma Physics and Controlled Fusion **44** (2002) 1815
[3] D. Post *et al* Physics of Plasmas **2** (1995) 2328
[4] A. Kallenbach *et al* 24th IAEA Fusion Energy Conf. (San Diego, CA, USA, Oct. 2012) ITR/P1-28
[5] J. W. Hughes *et al* Physics of Plasmas **9** (2002) 3019
[6] C. Giroud *et al* 24th IAEA Fusion Energy Conf. (San Diego, CA, USA, Oct. 2012) EX/P5-30
[7] M. N. A. Beurskens *et al* 24th IAEA Fusion Energy Conf. (San Diego, CA, USA, Oct. 2012) EX/P7-20
[8] S. I. Krasheninnikov *et al* Nuclear Fusion **27** (1987) 1805.